SURFACE MODIFICATION OF IRON OXIDE-MWCNTs NANOCOMPOSITE FOR POTENTIAL APPLICATION IN PHOTOCATALYSIS

Syahriza Ismail[1,*], Noor Farah Iddayu Abu Bakar[1], Noor Irinah Omar[1], Faisal Budiman[2] and Mohd Fadhil Majnis[3]

[1]Faculty of Industrial and Manufacturing Technology and Engineering, Universiti Teknikal Malaysia Melaka, Hang Tuah Jaya, 76100 Durian Tunggal, Melaka, Malaysia
[2]School of Electrical Engineering, Telkom University, Jl. Telekomunikasi Terusan Buah Batu Bandung 40257, Indonesia
[3]School of Chemical Engineering, College of Engineering, Universiti Teknologi MARA (UiTM), 40450 Shah Alam, Selangor Darul Ehsan, Malaysia

*syahriza@utem.edu.my

Abstract. Iron oxide is a compound that exists in several forms such as FeO, Fe_2O_3, and Fe_3O_4. In this study, iron oxide was incorporated with multi-walled carbon nanotubes (MWCNTs) to create a nanocomposite material for photocatalysis. The interaction between carbon and iron oxide is to investigate to improve the efficiency and stability of nanocomposites as photocatalysts. This nanocomposite is made by depositing MWCNTs on an iron sheet after being oxidized at 400 °C for 60 or 120 minutes. By using a spin coating technique, carbon nanotubes weighing between 0.15 and 0.50 mg were coated on the iron oxide that is formed after the oxidation process. The morphological and structural characteristics of this nanocomposite are characterized using different characterization techniques, including Raman spectroscopy, UV-Vis spectroscopy, field emission scanning electron microscopy (FESEM), and X-ray diffraction (XRD). Based on the XRD analysis, the α-Fe_2O_3 structure was formed and FESEM images have shown that MWCNTs were successfully deposited onto the surface of α-Fe_2O_3 nanoleaves. When the photocatalytic activity of the nanocomposite was examined using aqueous methyl orange (MO), it was discovered that the quantity of MWCNTs deposited on the α-Fe_2O_3 nanoleaves affected the effectiveness of MO dye. After five hours of exposure, a composite with 0.25 mg of MWCNTs demonstrated superior photocatalytic activity, degrading MO dye by 64%. On the surface of the nanocomposite, MWCNTs aid in the production of reactive radical species like OH• and O_2• and lessen the recombination of photo-generated charge carriers. Because of this synergistic mechanism, the photocatalytic process is more efficient, which makes iron oxide nanocomposite a practical material for a range of environmental application.

Keywords: Iron oxide, nanocomposite, photocatalysis

Article Info

Received 12th January 2024
Accepted 24th May 2024
Published 12th June 2024

ISSN: 1823-7010, eISSN: 2600-7444

1. INTRODUCTION

In recent years, the escalating levels of environmental pollution without viable solutions have become a focal point of scientific inquiry. The increase in environmental issues, particularly the surge in wastewater discharge containing organic dyes, has raised concerns within society. Consequently, photocatalysis has garnered significant interest for its role in mitigating the degradation of diverse dyes and contaminants present in wastewater. This attention is due to its environmentally sustainable, cost-effective, and eco-friendly nature, making it a promising avenue for addressing water pollution challenges.

Various materials were explored to address water contamination issues through photocatalysis. Zinc oxide (ZnO) and titanium dioxide (TiO_2) are well-known photocatalysts and work efficiently in breaking down organic contaminants. Nevertheless, iron oxide does also demonstrate notable catalytic activity. Iron oxide nanostructures stand out as strong candidates for this application due to their large surface area, superior conductivity, and affordability [1]. There are three different types of iron oxide: hematite (α-Fe_2O_3), maghemite (c-Fe_2O_3), and wustite (FeO) [2]. Of these, α-Fe_2O_3 has the most advantageous properties, including a 2.1 eV band gap [3], non-toxicity, low cost, and strong chemical stability in aqueous solutions. Additionally, it has a wide range of uses in the cement industry, water splitting, gas detection, solar energy conversion, lithium-ion battery manufacturing, water purification, and pigmentation, attracting more attention to the manufacture of iron oxide nanoparticles in these fields.

To date, several synthetic methods have been created for α-Fe_2O_3 nanostructure production, including hydrolysis of iron salt, sol-gel, oxidation, and hydrothermal synthesis. Among these methods, thermal oxidation stands out for its low cost, simplicity, and robustness. Srivastava et al. [4] have noted that oxidation, as a straightforward annealing treatment, holds promise for commercial-scale production. Furthermore, nanostructured morphology can be finely tuned by adjusting the oxidation temperature and environment.

Despite the advantages the iron oxide produces through the oxidation process, the standalone iron oxide may not suffice to enhance the catalytic process due to the recombination generation of photo-induced electrons and holes [5]. The low quantum yield of the photo-oxidation reaction of α-Fe_2O_3 is the fundamental impediment preventing its practical application. Consequently, the coupling of iron oxide with other materials becomes essential to enhance and optimize the photocatalytic properties. Carbon-based materials are increasingly being utilized for the surface modification of iron oxide due to their unique properties and potential applications. These materials offer several advantages, such as chemical stability which contribute to the long-term performance and functionality of the structure, and versatility where they come in various forms, including carbon nanotubes, graphene, and carbon dots. This versatility allows for the selection of the most suitable material based on the desired characteristics and finally enhances the performance of photocatalysis. Hence, this work aims to construct a composite system comprising multi-walled carbon nanotubes (MWCNTs) to overcome the weakness of α-Fe_2O_3. The combination of these materials involves using MWCNTs as trapping agents to prolong the recombination of electrons. This extension of recombination helps to increase the absorption wavelength from UV to visible-light area, hence enhancing the creation and separation of photogenerated carriers in photocatalytic applications. The photocatalytic reaction mechanism of the Fe_2O_3-MWCNTs involves a series of processes where the interaction between the Fe_2O_3-MWCNTs leads to enhanced photocatalytic performance. When exposed to light (typically UV or visible light), iron oxide-MWCNTs nanocomposites absorb photons. The absorbed energy excites electrons from the valence band to the conduction band in the iron oxide. This light-induced excitation creates electron-hole pairs (e^--h^+) within the iron oxide. Electrons (e^-) move to the conduction band, leaving behind positively charged holes (h^+) in the valence band. The generated electrons and holes participate in surface reactions where electrons reduce adsorbed species (e.g., organic pollutants) on the iron oxide surface and holes oxidize water or other molecules, producing reactive oxygen species.

Carbon nanotubes possess distinctive physical and chemical properties that have captured significant attention in the industry today. Among the remarkable physical attributes of carbon nanotubes is their capability to achieve thickness down to a single atomic layer. Combining these features with the magnetic properties of iron oxides results in the creation of effective photocatalytic materials, particularly those beneficial for magnetic adsorbents and photocatalyst applications.

In this study, the integration of multi-walled carbon nanotubes with iron oxide was achieved through the spin coating technique to fabricate the nanocomposite. Spin coating stands as a well-established method for uniformly depositing carbon nanotubes onto various surfaces. Moreover, the thermal oxidation process employed on iron foil facilitates the creation of the α-Fe_2O_3 nanoleaf structure. The integration of MWCNTs, spin coating, and thermal oxidation adds novelty to this study, enabling the fabrication of a promising iron oxide-MWCNTs nanocomposite with enhanced efficiency and stability of as photocatalysts.

2. MATERIALS AND METHODS

The methodology of the study involved the synthesis and characterization of α-Fe_2O_3/MWCNTs nanocomposites for photocatalytic applications, highlighting their potential as efficient photocatalysts for the degradation of organic pollutants in wastewater treatment applications. Iron (Fe) foils with a 0.1 mm thickness were used as substrates for oxidation. The foils were cut into 1.0 cm x 2.0 cm and ultrasonically cleaned in acetone and ethanol for 10 minutes, followed by being rinsed in distilled water. Finally, the foils were dried using an air stream. The thermal oxidation method was used to grow the nanostructure oxide layer due to its simplicity and robustness to produce the α-Fe_2O_3. It was carried out by using the chamber furnace (Nabertherm) at room temperature with normal air. At this stage, the alumina boat containing the sample substrate was loaded into the middle of the furnace.

Two different oxidation durations (90 and 120 °C) were performed at constant temperature to determine the optimum time required for the formation of α-Fe_2O_3. The MWCNTs obtained from CNano Technology have an average length and diameter of 10 µm and 11 nm, respectively and purity over 95%. These nanotubes were then chemically functionalized with –COOH groups using HNO_3 to improve their properties. As for the nanocomposite formation, different solvents were used to disperse 0.25 mg/ml MWCNTs. The solvents were dimethylformamide (DMF), acetone and sodium dodecyl benzene sulfonate (SDBS). All the dispersions were sonicated for 10 minutes using an ultrasonic probe. During the formation of iron oxide/MWCNTs nanocomposites, spin coating processes were used to deposit the dispersed MWCNTs onto the iron oxide nanoleaves. The spinning time and acceleration were set at 120 seconds and 3000 rpm respectively. The process was run for five cycles to obtain a homogenous distribution on the iron oxide surface. Finally, after the spin coating process, the heat treatment was done on the nanocomposite to help improve adhesion between MWCNTs and the iron oxide. The degradation testing was performed using a germicidal UV-C 150 W lamp and UV radiation acting as a light source, which was positioned 20 cm away from the dye solution. A cooling fan was used to cool the chamber and temperature was kept at around 25 °C.

3. RESULTS AND DISCUSSION

Figure 1(a) and (b) showcases typical FESEM images of the as-prepared iron oxide nanoleaf structures subjected to different durations of thermal oxidation: 90 and 120 minutes at 400 °C. Images (i) depict the top-view surface morphology, while (ii) illustrate the cross-sectional structures. The coverage of nanoleaf growth is seen at 90 min and 120 min. However, full coverage of nanoleaf growth can be seen after 120 minutes of oxidation. Oxide nanoleaf formation was driven by stress accumulation during thermal oxidation. Rackauskas [6] describes the oxidation process through the diffusion of Fe ion to the surface of the substrate from grain boundaries to the tip by stacking faults and surface diffusion.

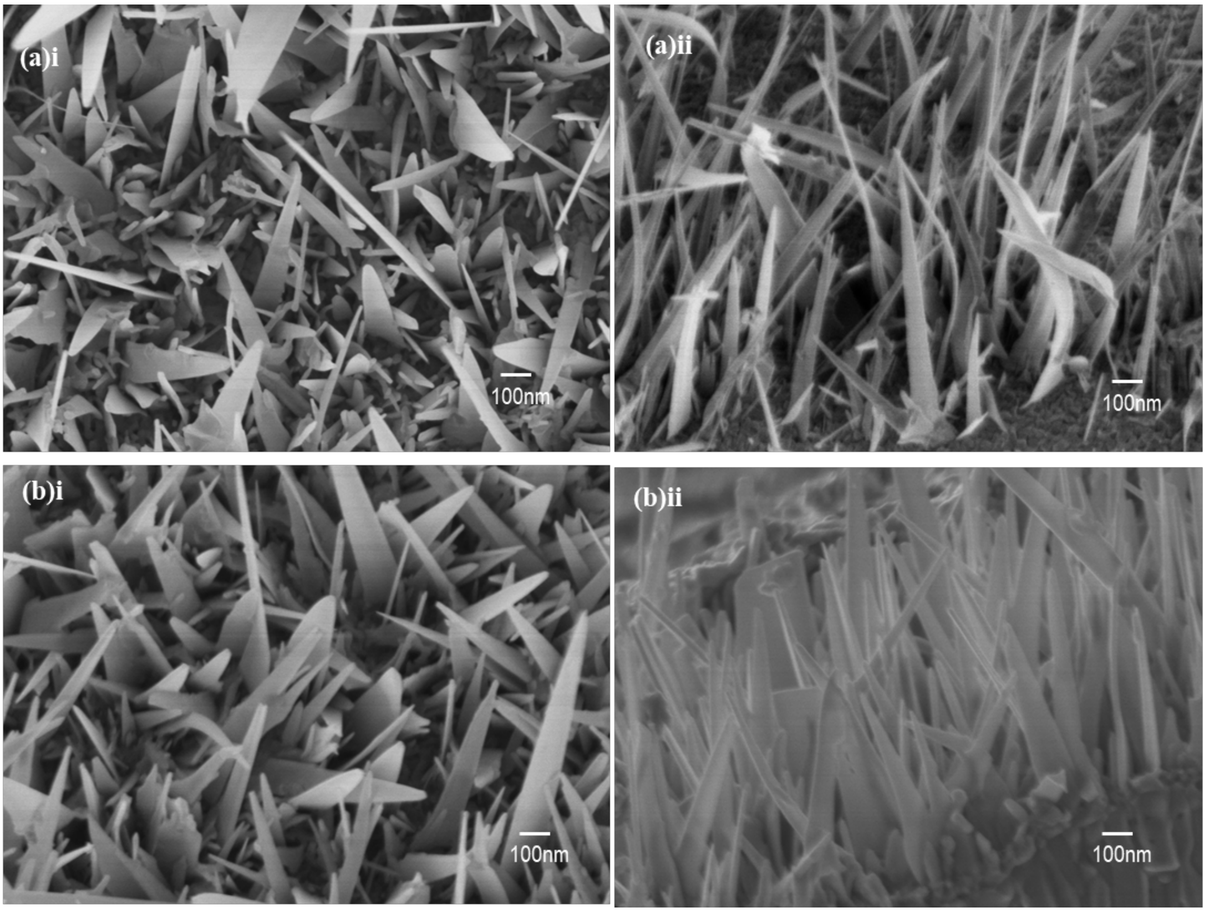

Figure 1: FESEM images of α-Fe_2O_3 nanowires formed by thermal oxidation at 400 °C for different durations: (a) 90 minutes and (b) 120 minutes. Images (i) show the top view, while (ii) show the cross-section morphologies

The iron oxide layer will eventually grow into a thin, sword-shaped structure with sharp points, resembling the leaves of corn plants, and the density of nanoleaf will increase on the substrate. The nanoleaf's uniformity in length, diameter, and tip size is a result of the variance in oxidation time. Additionally, because of the difference in diffusion rate, the growth of nanoleaf on the substrate also occurs in random areas [7].

XRD analysis was done to investigate the crystal structure of iron oxide and the result is shown in Figure 2. The XRD patterns reveal the presence of three iron oxide phases resembling the structures of iron (Fe), magnetite (Fe_3O_4), and hematite (α-Fe_2O_3). At the 90 minutes oxidation time, the transformation of peaks into hematite is not complete, primarily attributed to insufficient time and temperature to convert all oxide species into the hematite phase. At this stage, Fe peaks is also detected due to the removal of the nanowire structure. This structure comes from the Fe substrate itself, rather than the iron oxide layer. Figure 2 similarly demonstrates clear patterns, with the highest level of intensity observed in Fe_3O_4 and α-Fe_2O_3 after being oxidized for 120 minutes. The reason for this result can be attributed to the selective enhancement of the crystalline structure of hematite within the layer of oxidation that is generated during this phase. Simultaneously, the substrate peak of Fe at 44.67° and the peak at 65.02°, both at 120 minutes, start to decrease indicating an increased thickness of the oxide sample, which has mainly undergone complete oxidation

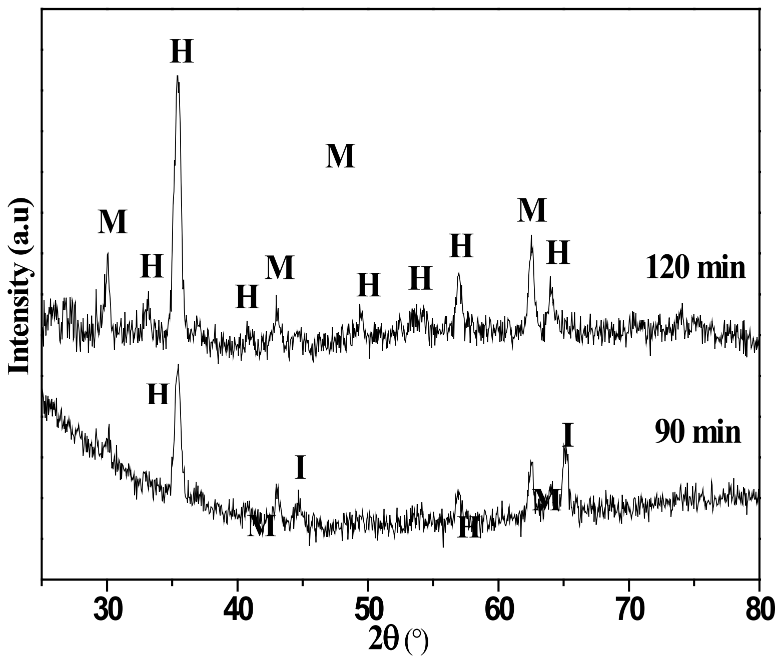

Figure 2: XRD patterns for iron oxide substrates formed via thermal oxidation at 400 °C for durations of 90 and 120 minutes. "Fe" denotes iron, while "M" and "H" signify magnetite (Fe_3O_4) and hematite (α-Fe_2O_3), respectively

The presence of iron oxide phases was verified through Raman spectroscopy, as depicted in Figure 3. The Raman spectra exhibit the oxidation samples at 90 and 120 minutes at 400 °C. Notably, two distinct peaks (227 and 662 cm^{-1}) corresponding to α-Fe_2O_3 and Fe_3O_4 are evident in both samples, with no other detected phase observed. The intensity of the peak at 120 minutes signifies a complete conversion to hematite, the most stable phase in the oxidized layer, and exhibits an increase with prolonged oxidation time. At the lowest oxidation time (90 minutes), non-hematite iron, specifically magnetite or Fe_3O_4, is indicated in the oxide layer. Moreover, the prominent formation of hematite at longer oxidation times is attributed to the further oxidation of magnetite initially formed during shorter oxidation periods. Nevertheless, the contribution of peaks from the substrate (Fe) cannot be disregarded. The results closely align with the Raman shift of α-Fe_2O_3 phases reported by Zhong et al. [8].

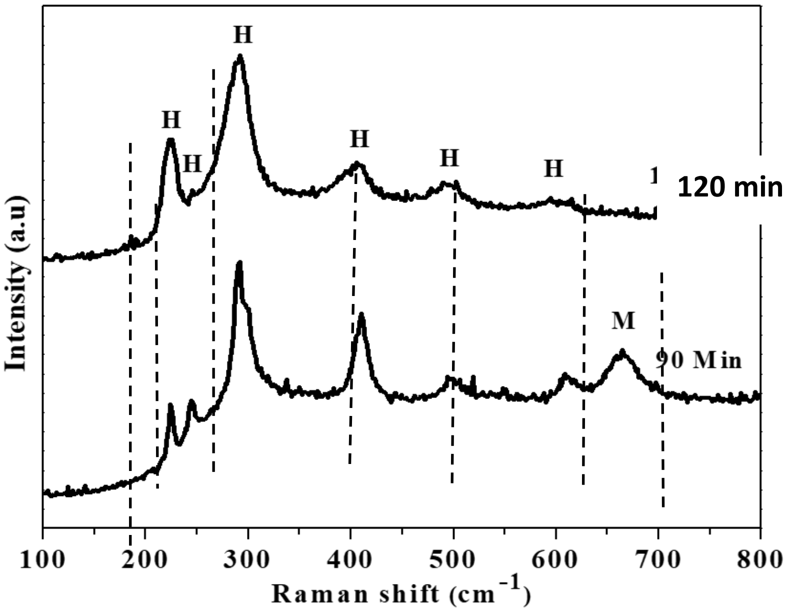

Figure 3: Raman spectra for iron oxide formed through thermal oxidation at 400 °C for various durations in air

The development of nanocomposite α-Fe_2O_3/MWCNTs is done by depositing MWCNTs on α-Fe_2O_3 by spin coating. During this deposition process, different solvents are used to disperse the MWCNTs before the spin coating process. The dispersion process is required in order to facilitate MWCNTs being evenly spread on the α-Fe_2O_3 substrate during the spin coating process. Thus, different solvents give different wettability interactions between MWCNTs and α-Fe_2O_3. Figure 4 shows the FESEM images of nanocomposite samples prepared by dispersing MWCNTs in different solvents.

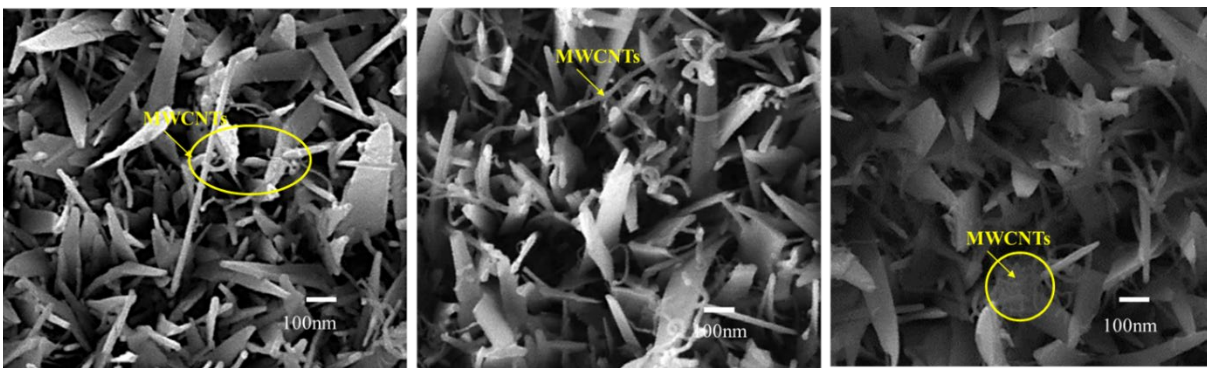

Figure 4: FESEM images of α-Fe_2O_3/MWCNTs nanocomposite dispersed in different solvent (a) acetone, (b) DMF and (c) SDBS

In Figure 4(a), the acetone solvent shows a well spread MWCNTs on the Fe_2O_3 nanostructure, but still has a small aggregate of MWCNTs on nanowires structure. Meanwhile, SDBS in water-soluble (Figure 4(c)) has shown an agglomeration of MWCNTs on the nanostructure. DMF solvent has shown a good distribution on the nanostructure. The coverage of MWCNTs on the nanoleaf structure when Acetone and DMF solvent is used has shown a good distribution due to the fact that the surface tension of both of solvents (DMF = 37.10 mN/m, Acetone = 25.20 mN/m) are lower and less than the critical surface tension of the iron oxide substrate (107 mN/m) [9]. This will enhance wettability, resulting in lower contact angles. The high polar wettability of DMF facilitates rapid and uniform solution spreading during spinning. As per Choi et al. [10], the low surface tension of DMF at the liquid/solid interface enhances layer uniformity and promotes thin film coverage (see Figure 4(b)). Moreover, MWCNTs dispersion in DMF solvent is excellent, leading to nearly complete coverage and thin film formation due to its low hydrogen bond donation parameter (α), abundant free electron pair availability (β), and high solvatochromic parameter (π) [11]. Hence, DMF emerges as one of the optimal solvents for MWCNTs dispersion.

Assessing the photocatalytic efficacy of the samples (pristine α-Fe_2O_3, α-Fe_2O_3/MWCNTs 0.15 mg, α-Fe_2O_3/MWCNTs 0.25 mg, α-Fe_2O_3/MWCNTs 0.35 mg, and α-Fe_2O_3/MWCNTs 0.5 mg nanocomposites) involved the degradation of methyl orange dye under a UV light source. The dye is expected to adsorb onto the photocatalyst's surface and degrade in the presence of light. Figure 5 illustrates the dye concentration over time during degradation. Clearly, the concentration of methyl orange dye decreases gradually in the presence of the photocatalyst. Pristine α-Fe_2O_3 exhibits poor photocatalytic performance, with only 28% degradation efficiency over 5 hours of UV irradiation. This poor response is attributed to the rapid recombination rate in pure α-Fe_2O_3, leading to inadequate dye degradation [12]. Meanwhile, the degradation increase for the 0.15 sample is probably due to the saturation of adsorbed pollutants, reducing further degradation efficiency. With the small amount of MWCNTs the active site may be very limited. Moreover, as reaction time increases, more charge recombination occurs, diminishing degradation rates.

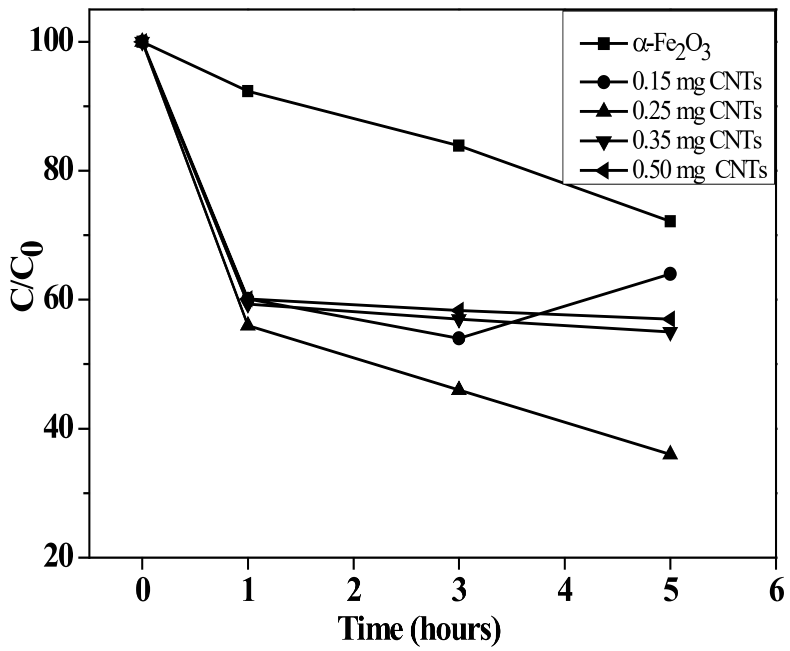

Figure 5: Degradadation of methyl orange over 5 hours

To address this issue and enhance degradation efficiency, researchers have explored the formation of nanocomposites. Incorporating carbon nanotubes (MWCNTs) into the composite significantly boosts degradation efficiency compared to pristine α-Fe_2O_3. Specifically, the addition of 0.25 mg of MWCNTs results in a notable 64% degradation, highlighting the favorable interaction between the nanowires and MWCNTs. This interaction leads to a uniform coating, indicative of the significant improvement in degradation performance. The outstanding photocatalytic activity can be attributed to the synergistic effects of iron oxide and carbon nanotubes (MWCNTs). As the band gap for this nanocomposite is altered due to the heterojunction between p-type MWCNTs and n-type Fe_2O_3 which helps reduce the recombination rate of photoinduced electron-hole pairs. The MWCNTs act as an electron sink, reducing the recombination rate of charge carriers. These components efficiently inhibit the recombination of photo-generated charge carriers and facilitate the generation of highly active radical species like OH• and O_2• radicals on the surface of the MWCNTs. However, when the MWCNTs content exceeds 0.25 mg, degradation performance decreases. This decline is attributed to excessive MWCNTs interacting with the nanoleaf, potentially obstructing UV light interaction with iron oxide. Consequently, the formation of electron-hole pairs through UV light interaction with iron oxide may be obstructed.

4. CONCLUSIONS

The thermal oxidation and spin coating methods were successfully synthesized the nanocomposite α-Fe_2O_3/MWCNTs. According to FESEM and XRD investigations, the nanocomposite is made up of α-Fe_2O_3 nanoleaf structure with MWCNTs lying on the leaf structure. The α-Fe_2O_3/MWCNTs composite exhibits a noteworthy enhancement in degradation efficiency when compared to pristine α-Fe_2O_3. The enhanced photocatalytic activity can be attributed to the synergistic effect of iron oxide and carbon nanotubes (MWCNTs), thus improving the overall photocatalytic performance. MWCNTs can facilitate the migration of excited electrons from the conduction band of Fe_2O_3 to electron acceptors on the MWCNTs surface, reducing electron-hole recombination and enhancing the degradation of pollutants. The presence of MWCNTs also lead to the formation of highly reactive radical species, such as hydroxyl radicals (•OH) and superoxide radicals (O_2•), on the MWCNTs surface. These radicals play a crucial role in the degradation of organic molecules in wastewater by initiating oxidation reactions.

Acknowledgements

The authors gratefully acknowledge Universiti Teknikal Malaysia Melaka for the financial support (short term grant S01871) and the Faculty of Industrial and Manufacturing Technology and Engineering for the laboratory's facilities.

”

Author Contributions

All authors contributed toward data analysis, drafting and critically revising the paper and agree to be accountable for all aspects of the work.

Disclosure of Conflict of Interest

The authors have no disclosures to declare.

Compliance with Ethical Standards

The work is compliant with ethical standards.

References

[1] Imran, M., Abutaleb, A., Ali, M. A., Ahamad, T., Ansari, A. R., Shariq, M. & Khan, A. (2020). UV light enabled photocatalytic activity of α-Fe_2O_3 nanoparticles synthesized via phase transformation. *Materials Letters*, 258, 126748.

[2] Aida, M. S., Alonizan, N., Zarrad, B. & Hjiri, M. (2023). Green synthesis of iron oxide nanoparticles using Hibiscus plant extract. *Journal of Taibah University for Science*, 17(1), 2221827.

[3] Valenzuela, M. A., Bosch, P., Jiménez-Becerrill, J., Quiroz, O. & Páez, A. I. (2002). Preparation, characterization, and photocatalytic activity of ZnO, Fe_2O_3 and $ZnFe_2O_4$. *Journal of Photochemistr y and photobiology A: Chemistry*, 148(1-3), 177-182.

[4] Srivastava, H., Tiwari, P., Srivastava, A. K. & Nandedkar, R. V. (2007). Growth and characterization of α-Fe_2O_3 nanowires. *Journal of Applied Physics*, 102(5), 054303.

[5] Mohamed, H. H., Alomair, N. A., Akhtar, S. & Youssef, T. E. (2019). Eco-friendly synthesized α-Fe_2O_3/TiO_2 heterojunction with enhanced visible light photocatalytic activity. *Journal of Photochemistry and Photobiology A: Chemistry*, 382, 111951.

[6] Rackauskas, S. (2011). Non-catalytic growth of metal oxide nanowires: properties and growth mechanism investigations. [Aalto University publication series Doctoral Dissertations]. Institutional repository of Aalto University.

[7] Rothman, A., Dubrovskii, V. G. & Joselevich, E. (2020). Kinetics and mechanism of planar nanowire growth. *Proceedings of the National Academy of Sciences*, 117(1), 152-160.

[8] Pattanayak, N., Kumar, J., Patra, P. P., Kumar, G. P. & Bajpai, A. (2021). Signatures of spin-phonon coupling in hematite crystallites through dielectric and Raman spectroscopy. *Europhysics Letters*, 134(4), 47003.

[9] Arkles, B. (2011). Hydrophobicity, hydrophilicity and silane surface modification. *Gelest Inc*, 215, 547-1015.

[10] Zhu, D. & Verduzco, R. (2020). Ultralow surface tension solvents enable facile COF activation with reduced pore collapse. *ACS applied materials & interfaces*, 12(29), 33121-33127.

[11] Gao, C., Guo, M., Liu, Y., Zhang, D., Gao, F., Sun, L., Li, J., Chen, X., Terrones, M. & Wang, Y. (2023). Surface modification methods and mechanisms in carbon nanotubes dispersion. *Carbon*, 118133.

[12] Lassoued, A. (2021). Synthesis and characterization of Ni-doped α-Fe_2O_3 nanoparticles through co-precipitation method with enhanced photocatalytic activities. *Journal of Materials Science. Materials in Electronics*, 29(7), 5726-5737.